



Title	Transcriptomic analysis of Porphyromonas gingivalis-infected head and neck cancer cells: Identification of PLAU as a candidate prognostic biomarker
Author(s)	Hamada, Masakazu; Inaba, Hiroaki; Nishiyama, Kyoko et al.
Citation	Journal of Cellular and Molecular Medicine. 2024, 28(4), p. JCMM18167
Version Type	VoR
URL	https://hdl.handle.net/11094/95670
rights	This article is licensed under a Creative Commons Attribution 4.0 International License.
Note	

The University of Osaka Institutional Knowledge Archive : OUKA


<https://ir.library.osaka-u.ac.jp/>

The University of Osaka

ORIGINAL ARTICLE

WILEY

Transcriptomic analysis of *Porphyromonas gingivalis*-infected head and neck cancer cells: Identification of PLAU as a candidate prognostic biomarker

Masakazu Hamada¹  | Hiroaki Inaba² | Kyoko Nishiyama¹ | Sho Yoshida² | Yoshiaki Yura¹ | Michiyo Matsumoto-Nakano² | Narikazu Uzawa¹

¹Department of Oral & Maxillofacial Oncology and Surgery, Osaka University Graduate School of Dentistry

²Department of Pediatric Dentistry, Okayama University Graduate School of Medicine, Dentistry and Pharmaceutical Sciences, Okayama, Japan

Correspondence

Masakazu Hamada, Department of Oral & Maxillofacial Oncology and Surgery, Osaka University Graduate School of Dentistry, 1-8 Yamadaoka, Suita, Osaka 565-0871, Japan.
Email: hamada.masakazu.dent@osaka-u.ac.jp

Funding information

Japan Society for the Promotion of Science, Grant/Award Number: 20K09918, 21K10111, 22K17202 and 23K09137

Abstract

Periodontal disease is a risk factor for head and neck squamous cell carcinoma (HNSCC), and *Porphyromonas gingivalis*, a major periodontal pathogen, has been identified as a specific and potentially independent microbial factor that increases the risk of cancer mortality. Gene expression in HNSCC due to *P. gingivalis* infection and how changes in gene expression affect the prognosis of HNSCC patients are not clarified. When *P. gingivalis* was cultured with HNSCC cells, it efficiently adhered to these cells and enhanced their invasive ability. A transcriptome analysis of *P. gingivalis*-infected HNSCC cells showed that genes related to migration, including CCL20, CITED2, CTGF, C8orf44-SGK3, DUSP10, EGR3, FUZ, HBEGF, IL1B, IL24, JUN, PLAU, PTGS2, P2RY1, SEMA7A, SGK1 and SIX2, were highly up- or down-regulated. The expression of up-regulated genes was examined using the expression data of HNSCC patients obtained from The Cancer Genome Atlas (TCGA) database, and the expression of 5 genes, including PLAU, was found to be higher in cancer tissue than in solid normal tissue. An analysis of protein–protein interactions revealed that these 5 genes formed a dense network. A Cox regression analysis showed that high PLAU expression levels were associated with a poor prognosis in patients with TCGA-HNSCC. Furthermore, the prognostic impact correlated with tumour size and the presence or absence of lymph node metastasis. Collectively, these results suggest the potential of PLAU as a molecular prognostic marker in HNSCC patients. Further in vivo and in vitro studies are needed to verify the findings of this study.

KEYWORDS

head and neck squamous cell carcinoma, migration, *P. gingivalis*, PLAU, RNA sequencing, TCGA

Masakazu Hamada, Hiroaki Inaba and Kyoko Nishiyama contributed equally to this work.

This is an open access article under the terms of the [Creative Commons Attribution](https://creativecommons.org/licenses/by/4.0/) License, which permits use, distribution and reproduction in any medium, provided the original work is properly cited.

© 2024 The Authors. *Journal of Cellular and Molecular Medicine* published by Foundation for Cellular and Molecular Medicine and John Wiley & Sons Ltd.

1 | INTRODUCTION

Head and neck cancer refers to cancers that develop in the hypopharynx, oropharynx, lip, oral cavity, nasopharynx or larynx, and is the sixth most common malignancy worldwide.^{1,2} Head and neck squamous cell carcinoma (HNSCC) accounts for 90%–95% of head and neck cancers.³ The main risk factors for HNSCCs are long-term smoking (including cigarettes, cigars and pipes), alcohol consumption and infection with high-risk types of human papillomavirus (HPV).^{4,5}

In recent years, microorganisms have also been implicated in carcinogenic mechanisms. *Helicobacter pylori* infection is the strongest known risk factor for gastric cancer and precedes cancer development.^{6–8} Periodontitis has been strongly associated with orodigestive cancer mortality, while *Porphyromonas gingivalis*, a major periodontal pathogen, was identified as a specific and potentially independent microbial factor that increases the risk of orodigestive cancer mortality.^{9–11} In addition, *Fusobacterium nucleatum*, which plays a role in periodontal disease, has been shown to play a role in the development and progression of colorectal cancer.^{12,13} We previously reported that *P. gingivalis* induced the production of the precursor form of matrix metalloproteinase-9 (proMMP-9) via proteinase-activated receptor (PAR)-related pathways, after which proMMP-9 was activated by gingipains to enhance the cellular invasion of HNSCC cells,^{14–16} while *F. nucleatum* was not.^{14,16} Furthermore, Ha et al. indicated the involvement of *P. gingivalis* infection in promoting the invasive potential of oral squamous cell carcinoma (OSCC) cells via the up-regulation of IL-8 and MMPs.¹⁷ However, it currently remains unclear whether the only relevant genes are those involved in signalling pathways, such as MMPs, ERK, p38 and PAR2/NFκB. It is not clear how *P. gingivalis*, with its ability to promote the invasive potential of HNSCC cells, affects the expression of other cellular genes involved in cell motility, that is, migration and invasion.

Recent studies revealed a major advance in consolidating the findings from extensive genetic analyses of HNSCC.^{18–22} In 2015, the Cancer Genome Atlas (TCGA) Network reported the comprehensive genomic characterization of HNSCC.²² The contribution of a broader landscape and frequency of chromosomal alterations and mutations as well as gene expression profiles to the aetiology, prognosis and treatment resistance of HNSCC was demonstrated by TCGA and other large-scale genomics studies.^{18–22} The potential of starvation-induced genes (SIGs), such as CALR, HSPA5 and TRIB3, as molecular prognostic markers has been proposed using the TCGA database of HNSCC patients.²³ Gene expression in HNSCC due to *P. gingivalis* infection and how changes in gene expression affect the prognosis of HNSCC patients are not clarified. Further efforts are needed to optimize the use of information in the TCGA-HNSCC database.

The effects of *P. gingivalis* on HNSCC patients were examined herein using omics analyses. The biological activity of HNSCC cells infected with *P. gingivalis* was assessed and their RNA was sequenced. Genes showing large fluctuations in their expression in vitro were extracted and subjected to an enrichment analysis. In addition, the

relationship between genes with an expression status affected by *P. gingivalis* infection and the prognosis of TCGA-HNSCC patients was investigated. Thereby, we attempted to clarify promising genes as predictor of HNSCC associated with *P. gingivalis* infection.

2 | MATERIALS AND METHODS

2.1 | Bacterial and cell cultures

The bacterial strain used was *P. gingivalis* ATCC 33277. Bacteria were grown in trypticase soy broth supplemented with yeast extract (1 mg/mL), menadione (1 µg/mL) and hemin (5 µg/mL), as previously described.¹⁴ The human HNSCC cell line HSC-3 was obtained from the RIKEN BRC CELL BANK (Tsukuba, Japan) and SAS cells from the Japanese Collection of Research Bioresources (Tokyo, Japan). Cultures were performed in RPMI 1640 medium (Sigma-Aldrich, St. Louis, MO) supplemented with 10% fetal bovine serum (FBS) at 37°C in a humidified atmosphere with 5% CO₂.

2.2 | Bacterial adhesion assay

Bacterial adhesion assays were performed as previously described.²⁴ SAS or HSC-3 cells were infected with bacteria at a multiplicity of infection (MOI) of 1 for 90 min and then washed with phosphate-buffered saline (PBS). To evaluate bacterial adhesion levels, cells were lysed with sterile distilled water for 15 min and dilutions of the lysate were plated and cultured anaerobically for CFU on blood agar supplemented with hemin and menadione.

2.3 | Cell invasion assay

Cell invasion was assessed by measuring the rate of migration of SAS and HSC-3 cells with the BD Matrigel™ Invasion Chamber (BD Biosciences, Bedford, MA). Cells (1.0×10^5) with or without *P. gingivalis* were seeded into the upper chambers in serum-free medium, while the lower wells were filled with RPMI1640 containing 10% FBS. After the incubation, non-invading cells were removed from the upper wells, and cells that had transferred to the inverse surface of the membrane were stained with 0.1% crystal violet. All experiments were completed in triplicate and six fields/well were counted. The invasion rate was expressed as the percentage of cells that passed through the matrigel membrane relative to migration through the control membrane (100%).

2.4 | Immunoblot analysis

SAS and HSC-3 cells were solubilized in cell lysis/extraction reagent (Sigma-Aldrich, St Louis, MO) containing a protease and phosphatase inhibitor cocktail (Thermo Scientific, Rockford, IL).

Immunoblotting was performed as previously described.¹⁴ Blots were probed with anti-CCL20 (Thermo Scientific, Rockford, IL) and anti-plasminogen activator urokinase (PLAU) (GeneTex International Corporation, Irvine, CA), and were reacted at 4°C overnight. The secondary antibody was alkaline phosphatase coupled with anti-rabbit IgG (Cell Signalling Technology, Danvers, MA). Reactions were developed with the 5-bromo-4-chloro-3-indolyl phosphate/nitroblue tetrazolium reaction. Blots were stripped and probed with an anti- β -actin antibody (Cell Signaling Technology) as a loading control.

2.5 | Enzyme-linked immunosorbent assay (ELISA) analysis

Sandwich ELISA kits were used to assess the concentrations of IL-17 (R&D System Inc., Minneapolis, MN) and TNF- α (R&D System Inc, Minneapolis, MN) according to the manufacturers' protocols. The SH-1000 Lab microplate reader (Corona Electric, Ibaraki, Japan) was used to measure absorbance at 450nm, with corrections to 550nm.

2.6 | RNA extraction

TRIsure (BIOLINE, Luckenwalde, Germany) was used according to the manufacturer's instructions to isolate total RNA from infected or control SAS cells. Two control samples and one 2-h sample were prepared.

2.7 | RNA sequencing and FASTQ file processing

The TruSeq stranded mRNA sample prep kit (Illumina, San Diego, CA) was used according to the manufacturer's protocol for library preparation. The Illumina HiSeq 2500 platform was used in the 75-base single-end mode for whole transcriptome sequencing. Base calling was performed using Illumina Casava ver.1.8.2 software. TopHat ver. 2.0.13 in combination with Bowtie2 ver. 2.2.3 and SAMtools ver. 0.1.19 mapped sequenced reads to human reference genome sequences (hg19). Cufflinks ver. 2.2.1 was used to calculate counts per gene. The median of the geometric means of fragment counts in all libraries was used to scale FPKMs and fragment counts.

2.8 | Analysis of normalized count data

Normalized counts were imported into Subio Platform v1.24.5853 (Subio Inc., Aichi, Japan),²⁵ which was used for all analyses. We set the lower limit by replacing positive numbers less than 10 with 10 and 0 counts with 8. The log₂ ratio was then calculated against the geometric mean of two control samples. Genes with counts <15 or log₂ ratios between -0.5 and 0.5 in all samples were filtered out,

which left 6363 genes. Candidate DEGs were extracted using the twofold criterion.

2.9 | Analysis of TCGA-HNSC RNA-Seq data

The RNA-Seq count data of TCGA-HNSC obtained from the GDC Data Portal²⁶ were analysed with the Subio platform. The workflow of TCGA RNA-Seq only differed from that applied to our RNA-seq data by the thresholds used. The lower limits for positive and 0 counts were 50 and 32, respectively, while the filters on counts and log₂ ratios were 50 and between -1 and 1, respectively. Log ratios were taken against the average of solid normal tissue samples. To compare survival times using the Kaplan–Meier method for each of the 17 selected genes, primary tumour samples were divided into those with count values higher or lower than the median.

2.10 | Pathway and protein–protein interaction analyses

The Database for Annotation, Visualization, and Integrated Discovery server was employed for the molecular pathways of the 17 selected genes to investigate their gene ontology (GO) terms and Kyoto Encyclopedia of Genes and Genomes (KEGG) pathways. A GO enrichment analysis was performed over the following primary levels: cellular components (CC), biological processes (BP), and molecular functions (MF). A protein–protein interaction (PPI) network was established using these genes according to the STRING online database (<https://string-db.org/>). We visualized the most significant modules in PPI networks.

2.11 | Statistical analysis

Student's *t*-test was performed using Microsoft Excel (Microsoft, Redmond, WA, USA). Results are shown as the mean \pm SD. The significance of differences was set at $p < 0.05$.

The effects of PLAU gene expression (low vs. high) on all-cause mortality was examined by a Cox proportional hazards model analysis, with PLAU gene expression as the independent variable. To correct for known risk factors, including age, sex, the HPV status, alcohol consumption, smoking (cigarettes per day) and the M, N and T stages, multivariate models were constructed with these factors also as independent variables. The proportional hazard nature of PLAU gene expression was confirmed by double log plots.

Furthermore, a Kaplan–Meier curve and the Log-rank test using gene expression as a factor, stratified by known risk factors, were used to confirm interactions with known risk factors. Regarding interaction factors that showed significance, a Cox proportional hazards model including the interaction term was constructed to verify the effects of the interaction after corrections for confounding factors.

All statistical analyses were performed with SPSS version 24.0 for Windows (IBM Japan, Tokyo, Japan). All *p*-values were two-tailed; $p < 0.05$ was considered to be significant.

3 | RESULTS

3.1 | Effects of *P. gingivalis* on the biological activity of HNSCC cells

We investigated the mechanisms underlying the responses of HNSCC cells infected with *P. gingivalis* and *F. nucleatum*. SAS cells and HSC-3 cells were cultured with *P. gingivalis* or *F. nucleatum* at a MOI of 1 for 90 min. *P. gingivalis* was shown to adhere to SAS cells and HSC-3 cells at significantly greater levels than *F. nucleatum* (Figure 1A,B). We previously reported on the use of matrigel-coated transwell membranes to determine whether the adhesion efficiency of oral bacteria was related to the invasive capability of HNSCC

cells.¹⁴ We found that cellular invasion was greater by SAS cells infected with *P. gingivalis* than by those infected with *F. nucleatum* (Figure 1C). These results are consistent with our previous finding of OSCC invasion mediated by *P. gingivalis*.¹⁴

3.2 | RNA sequencing of SAS cells infected with *P. gingivalis* and changes in the expression of genes related to migration

Based on the results obtained on the biological activity of HNSCC cells infected with *P. gingivalis*, *P. gingivalis*-infected SAS cells were subjected to RNA sequencing with or without *P. gingivalis* at a MOI

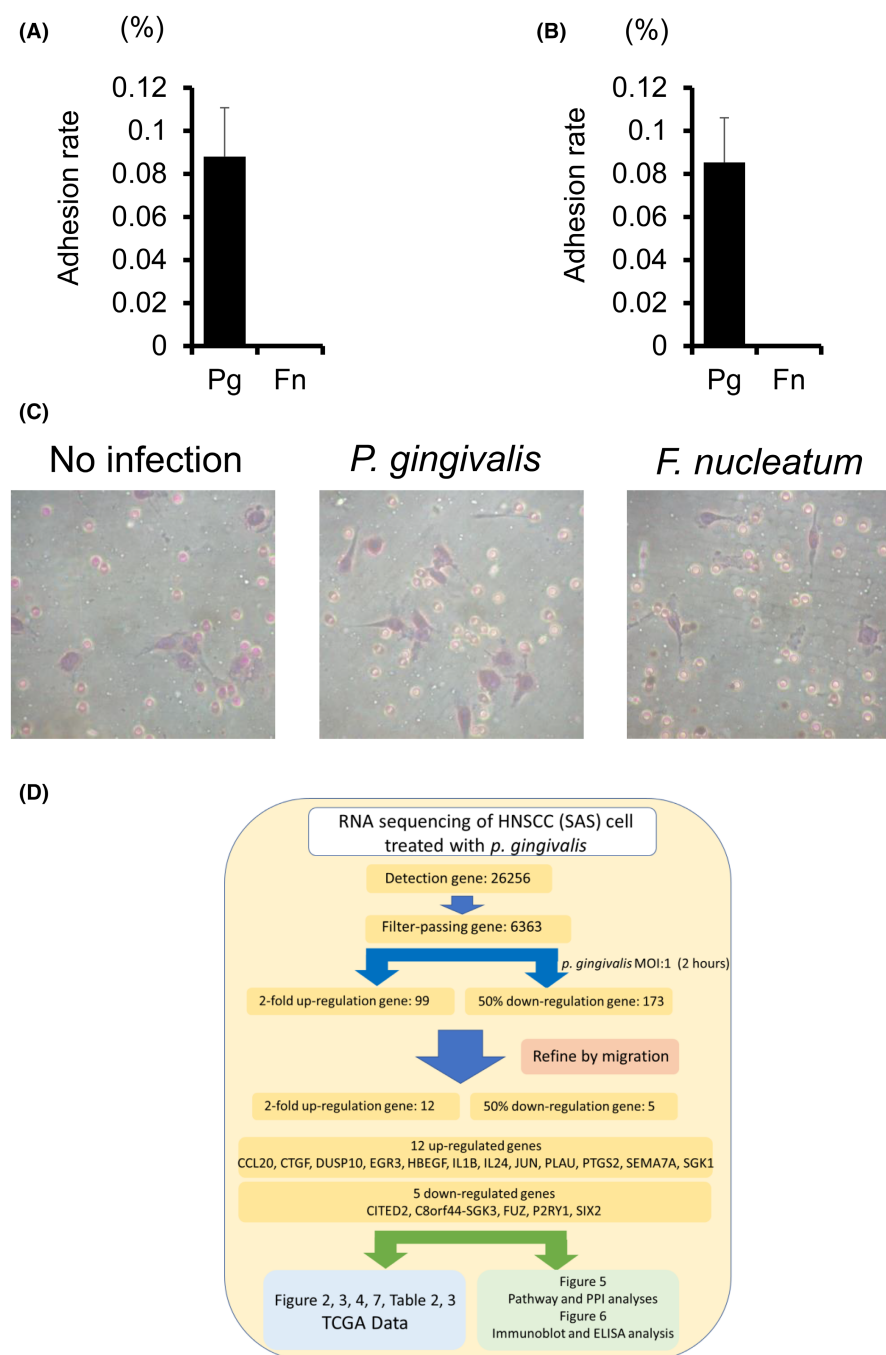


FIGURE 1 Effects of *P. gingivalis* on the biological activity of HNSCC cells. SAS cells (A) and HSC-3 cells (B) were cultured with *P. gingivalis* or *F. nucleatum* at a MOI of 1 for 90 min. MOI 1 of *P. gingivalis* showed that adhesion to cancer cells was possible. Data are shown as the mean \pm SD of 3 independent experiments and analysed by the t-test. (C) SAS cell and HSC-3 cell invasion through matrigel-coated transwell membranes was assessed 24 h after *P. gingivalis* infection. (D) The schedule of the RNA sequencing of SAS cells after *P. gingivalis* infection.

of 1 for 2 h and genes showing large fluctuations in their expression were extracted. Since *P. gingivalis* is known to affect both invasion and migration,²⁷ we focused on migration, which has the most extractable genes. Figure 1D shows the schedule of these experiments. After the infection of cells with *P. gingivalis* for 2 h, a more than two-fold increase in expression was observed for 99 genes. Among them, 12 migration-related genes, including CCL20, CTGF, DUSP10, EGR3, HBEGF, IL1B, IL24, JUN, PLAU, PTGS2, SEMA7A and SGK1, were identified (Table 1). In contrast, a 50% reduction in expression was noted in 173 genes in response to *P. gingivalis* infection. Moreover, five genes, including CITED2, C8orf44-SGK3, FUZ, P2RY1, and SIX2, were associated with carcinoma migration (Table 1). Many of these genes were no longer altered after 24 h and the changes were transient (Table 1).

3.3 | Expression of 17 genes extracted from migration keywords in TCGA-HNSCC patients

Gene expression was examined in the tumour tissues of TCGA-HNSCC patients. We focused on 17 genes associated with migration in cells infected with *P. gingivalis*. In clinical samples analysed by TCGA, the expression of 5 genes, CCL20, IL1B, IL24, PLAU and SEMA7A, was significantly higher in the primary tumour than in solid normal tissue (Figure 2A), whereas that of CITED2 was lower (Figure 2B). A heat map was also created to represent the degree to which the expression of the 17 genes was up- or down-regulated (Figure 2C). The detailed clinical data breakdown of the TCGA-HNSCC 499 patients used in this study was as follows: alive ($n=282$; 56.5%), dead ($n=217$; 43.5%), alcohol yes ($n=332$; 66.5%), alcohol no ($n=156$; 31.3%), alcohol unknown ($n=11$; 2.2%), cigarettes yes ($n=286$; 57.3%), cigarettes no ($n=213$; 42.7%), HPV positive ($n=89$; 17.8%), HPV negative ($n=408$; 81.8%), HPV unknown ($n=2$; 0.4%), male ($n=367$; 73.5%), female ($n=132$; 26.5%), lymph node metastasis yes ($n=239$; 47.9%), lymph node metastasis no ($n=238$; 47.7%), lymph node metastasis unknown ($n=22$; 4.4%), tumour size T1-2 ($n=176$; 35.3%), tumour size $\geq T3$ ($n=308$; 61.7%), tumour size unknown ($n=15$; 3.0%). The heat map also included detailed clinical data on vital status, drinking, smoking, the HPV status, sex, the presence of lymph node metastasis and tumour size (Figure 2C).

3.4 | Prognostic significance of 17 genes extracted from migration keywords in TCGA-HNSCC patients

We investigated whether the 17 genes associated with migration listed in Table 1 affected the prognosis of patients. Patients were divided into two groups based on the high or low expression of these genes. Expression levels higher than the median were classified as the high expression group and the remainder as the low expression group.^{23,28,29} The generalized Wilcoxon test and Log rank test were performed to assess the differences in survival times identified by the Kaplan–Meier method (Figures 3 and 4). Among the 12 up-regulated

genes, the high expression of CCL20 (Figure 3A), HBEGF (Figure 3E), and PLAU (Figure 3I) correlated with shorter survival times, whereas the high expression of CTGF (Figure 3B), DUSP10 (Figure 3C), EGR3 (Figure 3D), IL1B (Figure 3F), IL24 (Figure 3G), JUN (Figure 3H), PTGS2 (Figure 3J), SEMA7A (Figure 3K) and SGK1 (Figure 3L) did not. Down-regulated genes were also examined using the Kaplan–Meier method, which revealed no relationship between gene expression and survival in TCGA-HNSCC patients (Figure 4A–E).

3.5 | Function and PPI analyses of 17 genes extracted from migration keywords

The biological properties and potential signalling pathways of the 17 selected genes were investigated using GO and KEGG enrichment pathway analyses. The GO enrichment analysis identified the following enriched terms: positive regulation of the ERK1/2 cascade, response to lipopolysaccharide, regulation of cell proliferation, negative regulation of cell migration, negative regulation of cell proliferation, aging, positive regulation of protein phosphorylation, positive regulation of cell migration, response to mechanical stimulus, positive regulation of transcription from RNA polymerase II promoter, signal transduction, positive regulation of fever generation, inflammatory response, positive regulation of prostaglandin biosynthetic process, positive regulation of cell proliferation and regulation of chondrocyte differentiation (Figure 5A). The KEGG analysis revealed the significant enrichment of prognostic genes in the following pathways: IL-17 signalling pathway, C-type lectin receptor signalling pathway, TNF signalling pathway, Leishmaniasis, Rheumatoid arthritis and NF-kappa B signalling pathway (Figure 5B). In the PPI network analysis, ATF2, ATF3, BATF3, CCL20, CREBBP, CTGF, CTNNB1, EP300, EGFR, EGR3, ERBB4, FOS, FOSB, FOSL1, FOSL2, GPR29, HBEGF, IL1R2, IL24, JUN, PLAU, PLAUR, PTGS2, SERPINE1, SMAD3 and VTN formed a close interaction network (Figure 5C).

3.6 | Expression levels of CCL20, PLAU, IL17 and TNF- α

The expression of CCL20 and PLAU significantly differed between primary tumours and solid normal tissues and in survival curves by the Kaplan–Meier method (Figure 3A,I). Therefore, we examined the expression of CCL20 and PLAU, and each was confirmed to be expressed in SAS cells. The most efficient expression level of PLAU in SAS cells was observed at 2 h following *P. gingivalis* infection, but its expression was decreased at 24 h (Figure 6A). In HSC-3 cells, basal levels of PLAU were higher than in SAS cells and were not specifically altered by *P. gingivalis* infection (Figure 6B). Similar expression levels were maintained in HSC-4 cells derived from HSC-3 cells (data not shown). Expression levels of CCL20 in SAS cells did not change with time (Figure 6A). We then examined the TNF- α and IL-17 signalling pathways extracted by the KEGG analysis (Figure 5B). ELISA

TABLE 1 Genes selected by the keyword migration and highly up- or down-regulated after *P. gingivalis* infection.

ID	Description	NCBI Gene ID	Fold Change after 2h	Fold Change after 24h
SGK1	Serum/glucocorticoid regulated kinase 1	6446	2.0548851	0.84200996
CTGF	Connective tissue growth factor	1490	2.103659	1.3085716
PLAU	Plasminogen activator, urokinase	5328	2.1137452	0.972356
IL24	Interleukin 24	11009	2.1794877	0.8333334
PTGS2	Prostaglandin-endoperoxide synthase 2	5743	2.4285715	0.4642857
CCL20	C-C motif chemokine ligand 20	6364	2.56447	0.5604719
JUN	Jun proto-oncogene, AP-1 transcription factor subunit	3725	2.7633407	1.1304604
IL1B	Interleukin 1 beta	3553	2.877408	1.4091259
SEMA7A	Semaphorin 7A (John Milton Hagen blood group)	8482	3.243119	1.3338866
HBEGF	Heparin binding EGF like growth factor	1839	3.4484425	0.7531739
DUSP10	Dual specificity phosphatase 10	11221	3.7250006	1.7719301
EGR3	Early growth response 3	1960	4.2445884	0.7156118
P2RY1	Purinergic receptor P2Y1	5028	0.48148143	0.59090906
SIX2	SIX homeobox 2	10736	0.4761905	1.3000001
CITED2	Cbp/p300 interacting transactivator with Glu/Asp rich carboxy-terminal domain 2	10370	0.42384875	1.1889815
FUZ	Fuzzy planar cell polarity protein	80199	0.33333337	0.7727273
C8orf44-SGK3	C8orf44-SGK3 read-through	100533105	0.29074886	0.6567796

showed that IL-17 production increased in SAS cells infected with *P. gingivalis* (Figure 6C), while TNF- α production remained unchanged (Figure 6D).

3.7 | Relationship of PLAU and classical prognostic factors with survival in TCGA-HNSCC patients

Since high PLAU expression correlated with shorter survival (Figure 3I) and increases in PLAU due to the *P. gingivalis* infection were also observed at the protein level (Figure 6A), the effects of drinking (Figure 7A,B), smoking (Figure 7C,D), the HPV status (Figure 7E,F), sex (Figure 7G,H), the presence of lymph node metastasis (Figure 7I,J), and tumour size (Figure 7K,L) on PLAU patient survival were examined. Survival curves were not affected by PLAU expression in the absence of lymph node metastasis (Figure 7J), but were markedly changed by its expression in cases with lymph node metastasis (Figure 7I). Furthermore, survival curves were not affected by PLAU expression in T1-T2 tumours

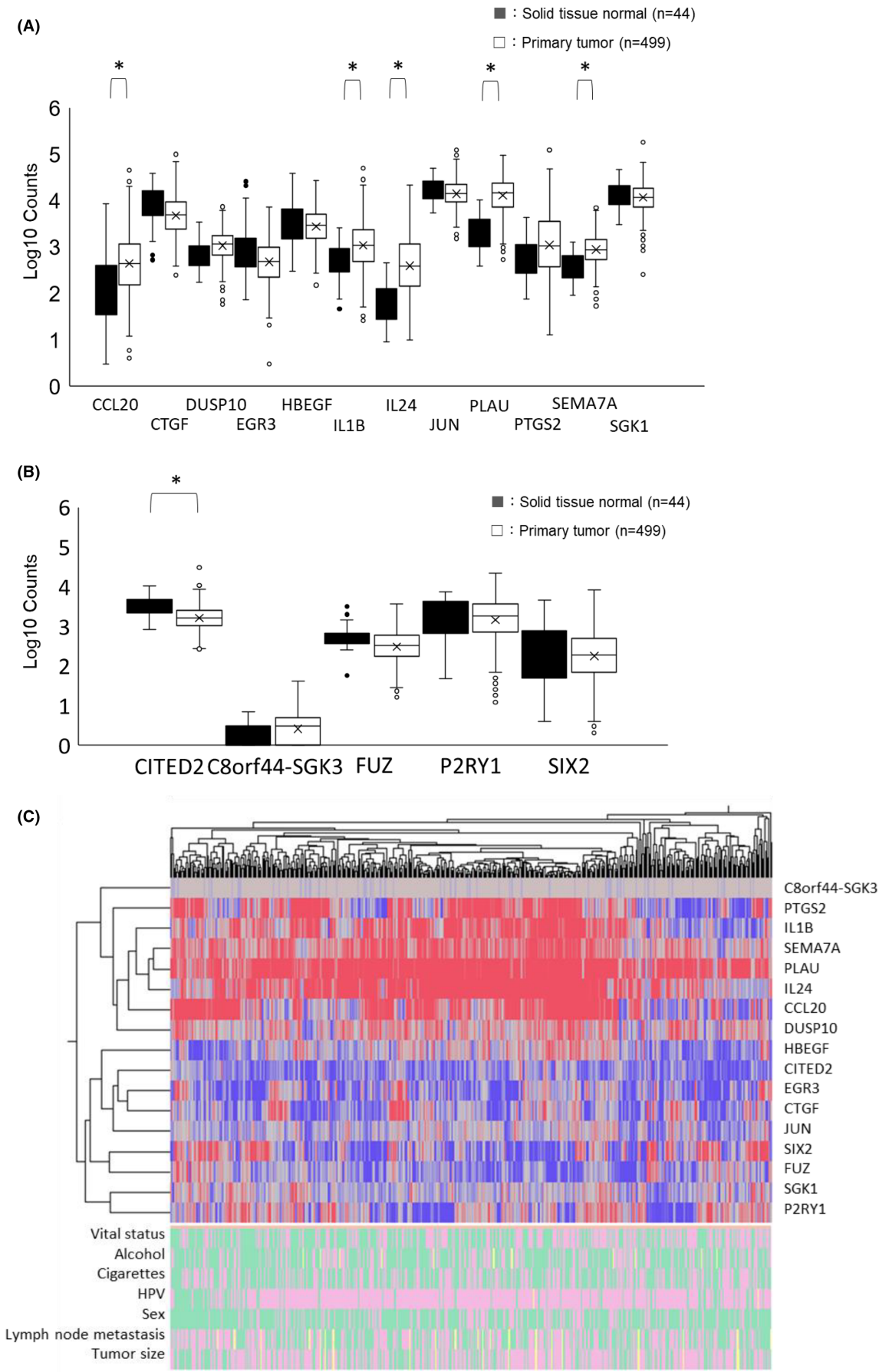
(Figure 7K), but were significantly changed by its expression in tumours \geq T3 (Figure 7L).

3.8 | Cox regression analysis of the relationship of PLAU and classical prognostic factors with survival in TCGA-HNSCC patients

Table 2 shows the effects of PLAU gene expression on all-cause mortality. The univariate analysis showed a higher risk of all-cause mortality in the high PLAU expression group than in the low PLAU expression group (hazard ratio [HR]=1.722 [95%CI: 1.294, 2.293], $p<0.001$). Among known risk factors, age, sex, the M stage and N stage correlated with all-cause mortality. The multivariate analysis to correct for confounding factors showed that high PLAU expression was a significant risk factor for all-cause mortality even after adjustments for known risk factors (HR=1.804 [95%CI: 1.331, 2.446], $p<0.001$).

A stratified Kaplan-Meier analysis suggested interactions between lymph node metastasis, tumour size and PLAU expression

FIGURE 2 RNA sequencing of SAS cells after *P. gingivalis* infection and changes in the expression of genes related to migration. The expression of 17 genes showed significant changes after *P. gingivalis* infection and they were extracted by migration keywords. Their relative expression levels in TCGA-HNSCC patients were assessed in primary tumours and solid normal tissues. (A) Box plots of the expression of 12 genes (CCL20, CTGF, DUSP10, EGR3, HBEGF, IL1B, IL24, JUN, PLAU, PTGS2, SEMA7A, and SGK1) showing more than two-fold increases in expression. (B) Box plots of the expression of 5 genes (CITED2, C8orf44-SGK3, FUZ, P2RY1, and SIX2) showing a 50% reduction in expression. (C) Heat map of the 17 gene expression profiles. Colours from blue to red indicate low to high expression levels. The detailed clinical data breakdown of the patients is as follows: alive (■), dead (■), alcohol yes (■), alcohol no (■), alcohol unknown (■), cigarettes yes (■), cigarettes no (■), HPV positive (■), HPV negative (■), HPV unknown (■), Male (■), Female (■), lymph node metastasis yes (■), lymph node metastasis no (■), lymph node metastasis unknown (■), tumour size T1-2 (■), tumour size \geq T3 (■), tumour size unknown (■).



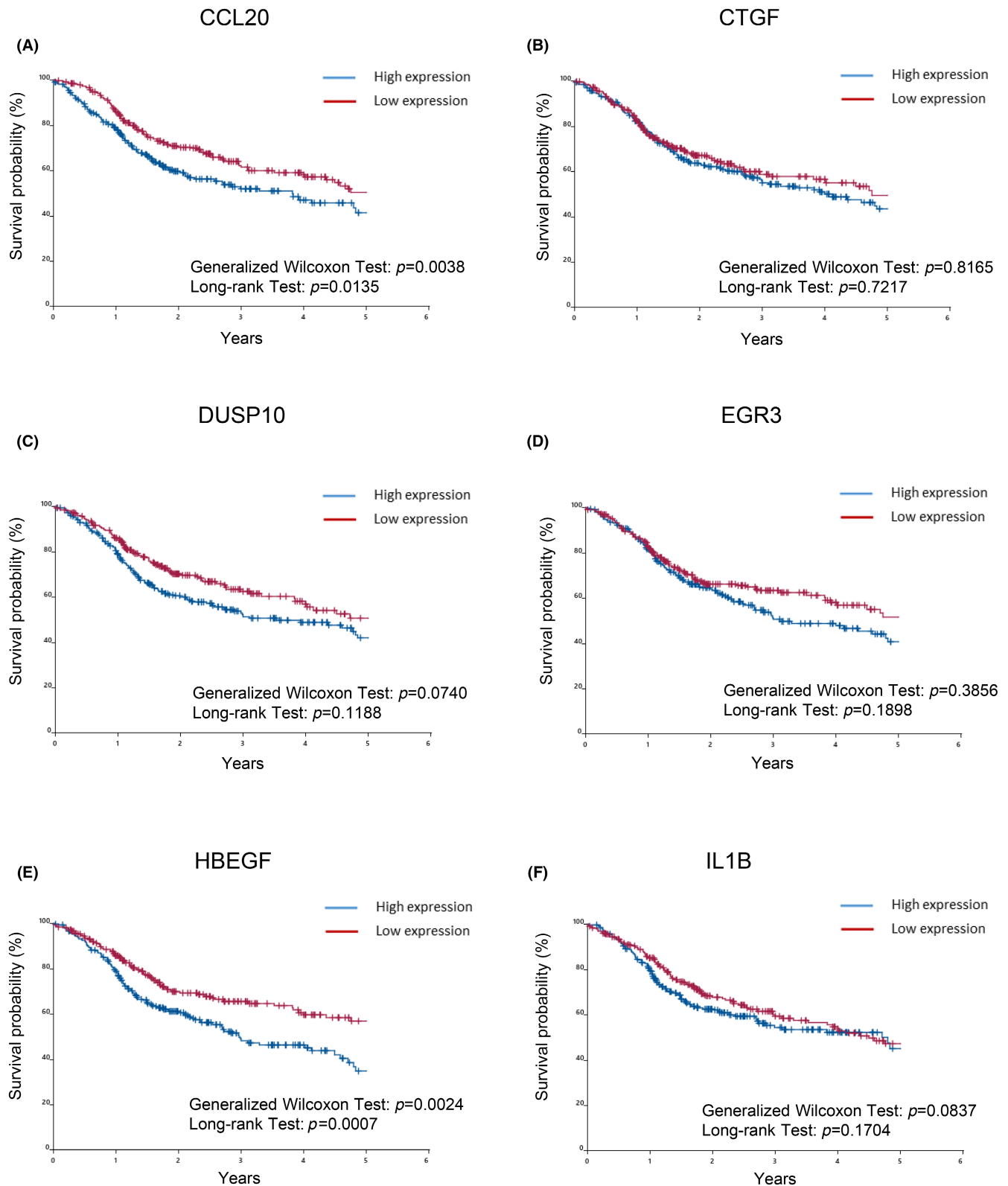


FIGURE 3 Prognostic significance of 12 up-regulated genes extracted from migration keywords in TCGA-HNSCC patients. The overall survival of TCGA-HNSCC patients, classified by 12 up-regulated genes extracted from migration keywords, was assessed by the Kaplan–Meier method. Differences in survival times measured by the Kaplan–Meier method were examined using the generalized Wilcoxon test and Log rank test. A: CCL20, B: CTGF, C: DUSP10, D: EGR3, E: HBEGF, F: IL1B, G: IL24, H: JUN, I: PLAUG, J: PTGS2, K: SEMA7A, L: SGK1.

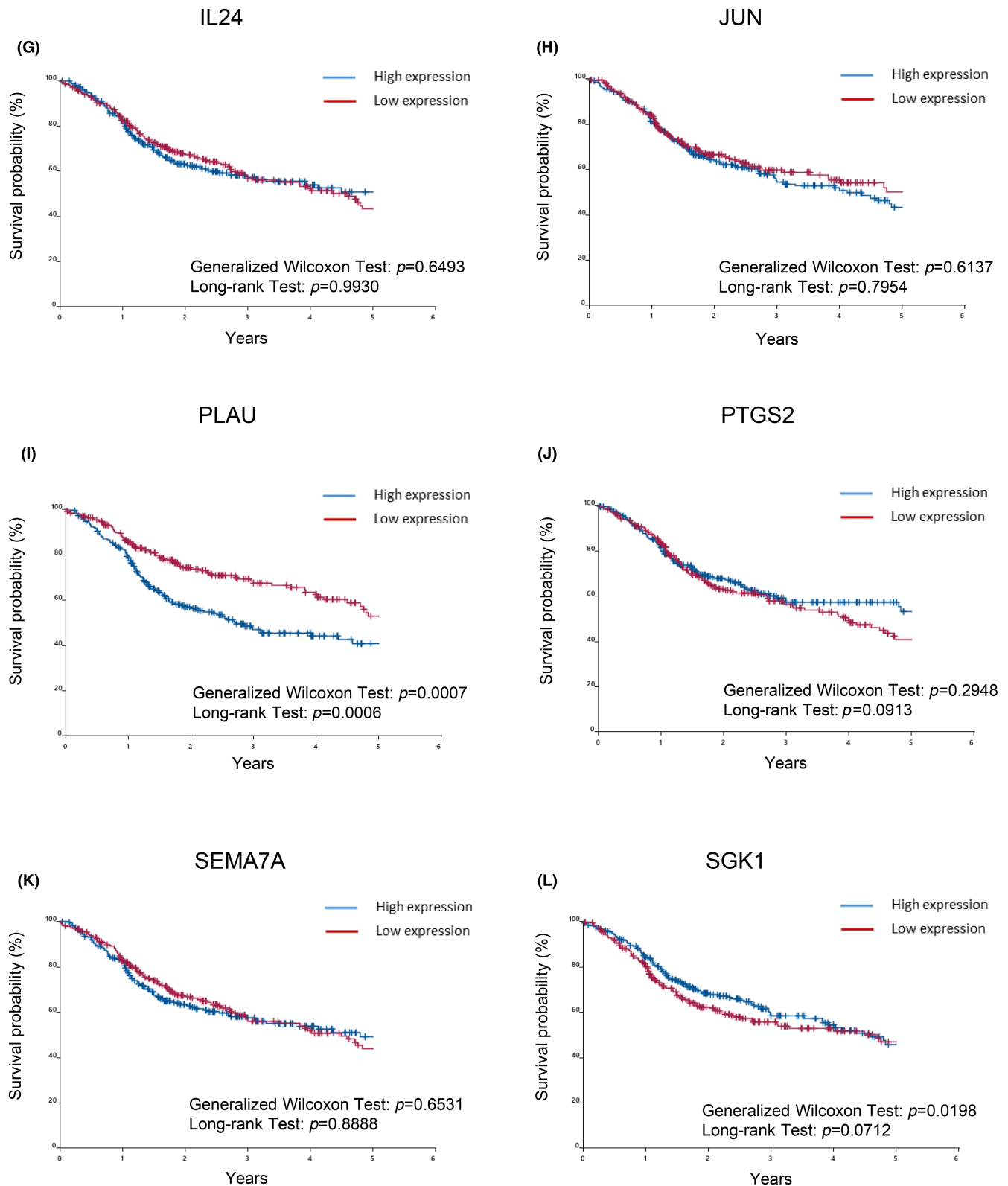


FIGURE 3 (Continued)

(Figure 7I–L). The results of the multivariate model testing these interaction terms under corrections for confounding factors are shown in Table 3.

The results of the interaction analysis with lymph node metastasis showed that PLAU expression was a significant factor affecting all-cause mortality only in the population with lymph node metastasis

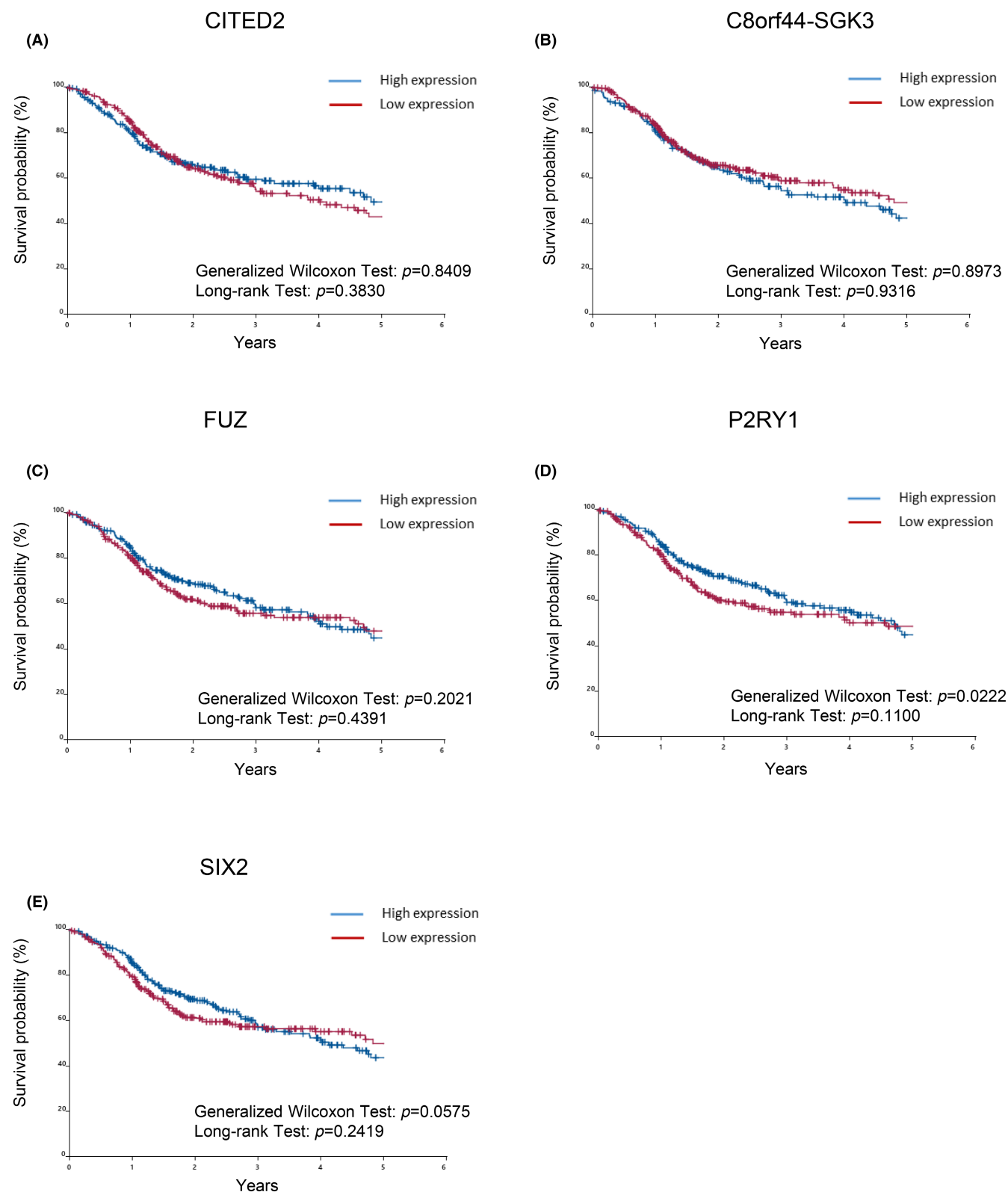
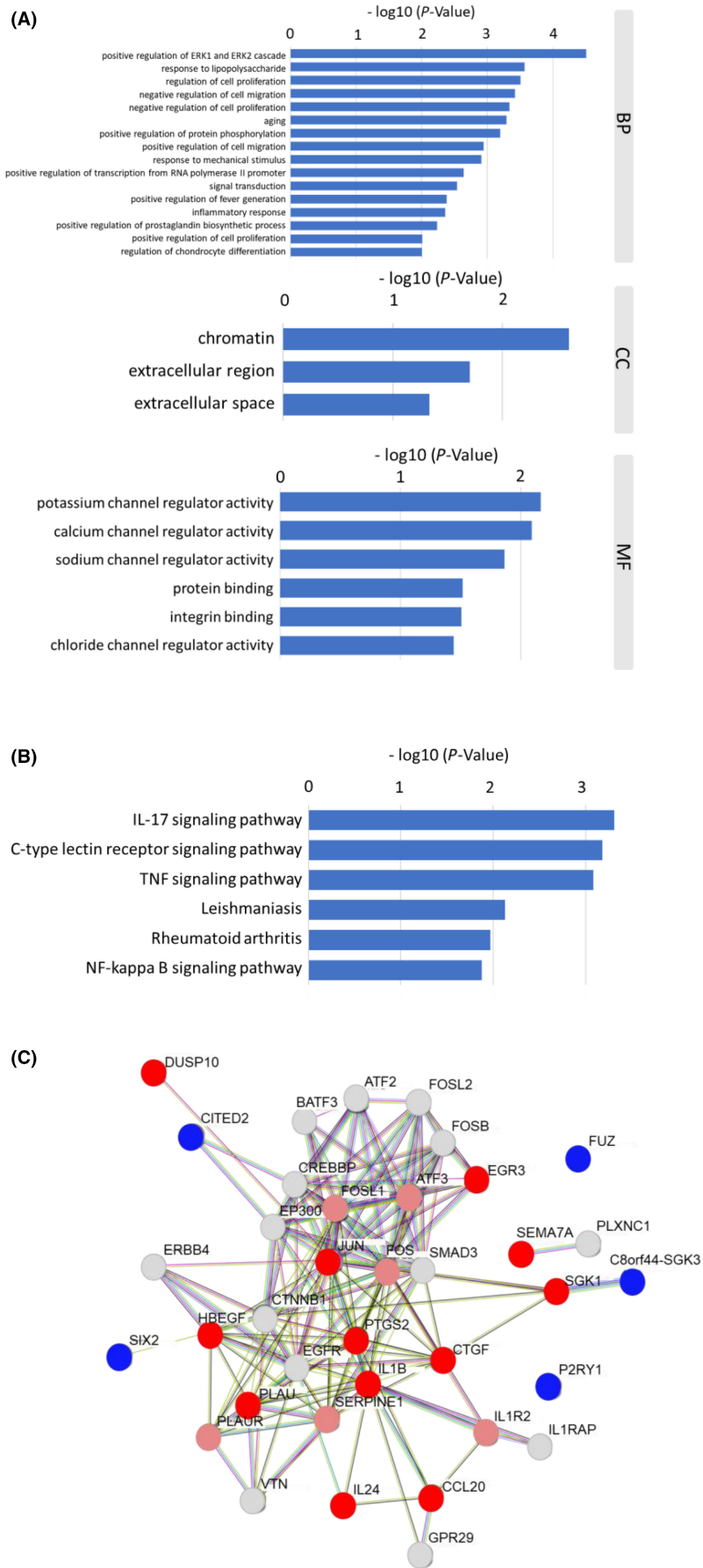


FIGURE 4 Prognostic significance of 5 down-regulated genes extracted from migration keywords in TCGA-HNSCC patients. The overall survival of TCGA-HNSCC patients, classified by 5 down-regulated genes extracted from migration keywords, was assessed by the Kaplan–Meier method. Differences in survival times measured by the Kaplan–Meier method were examined using the generalized Wilcoxon test and Log rank test. A: CITED2, B: C8orf44-SGK3, C: FUZ, D: P2RY1, E: SIX2.

FIGURE 5 Function and PPI analyses of 17 genes extracted from migration keywords. (A) A list of GO terms identified by the GO enrichment analysis of 17 selected genes. BP, biological process; CC, cellular composition; MF, molecular function. (B) List of molecular pathways identified by the KEGG pathway enrichment analysis of 17 selected genes. (C) Proteins encoded by 17 genes extracted from migration keywords were subjected to a PPI network analysis. Up-regulated genes are shown in red. Down-regulation is shown in blue, and grey indicates genes with expression levels that remained unchanged after *P. gingivalis* infection.



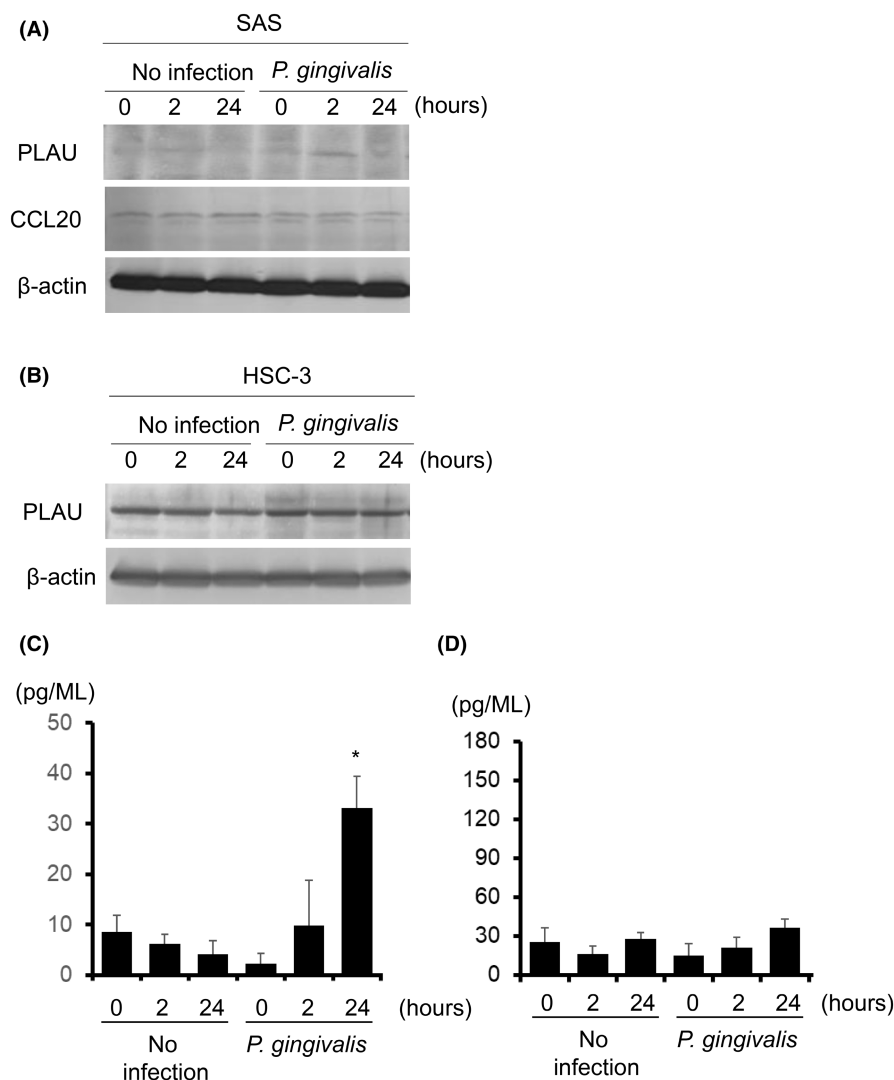


FIGURE 6 Expression levels of CCL20, PLAU, IL17, and TNF- α . Cells were incubated with *P. gingivalis* at a MOI of 1 for the indicated times, and lysates were subjected to immunoblotting. (A) PLAU and CCL 20 (SAS cells), (B) PLAU (HSC-3 cells). β -Actin was included as a loading control for whole cell lysates. ELISA showed IL-17 production (C) and TNF- α production (D) using SAS cells.

(HR=2.908 [95%CI: 1.864, 4.536], $p<0.001$), and the interaction term was also significant ($p=0.004$ [PLAU \times Lymph node metastasis]).

The results of the interaction analysis with tumour size showed that PLAU expression was a significant factor affecting all-cause mortality only in the population with a large tumour size ($\geq T3$) (HR=2.298 [95%CI: 1.595, 3.312], $p<0.001$), and the interaction term was also significant ($p=0.013$ [PLAU \times Tumour size]).

4 | DISCUSSION

Periodontitis, a bacterial gingival disease, is associated with a two- to fivefold higher risk of developing cancer, particularly *P. gingivalis* and *F. nucleatum*, which were found to be metastatic by several different mechanisms.^{30,31} In addition, periodontitis was also shown to be predictive of a 5.23-fold increase in the risk of tongue cancer.^{14,32} *P. gingivalis*, a major periodontal pathogen, has been identified as a specific and potentially independent microbial factor increasing the risk of orodigestive cancer mortality.^{16,33} In the present study, *P. gingivalis* adhered to HNSCC cells at significantly higher levels than *F. nucleatum* at the same MOI. We previously reported that *P. gingivalis*

promoted the migration and invasion of HNSCC cell lines through the induction and activation of proMMP9, whereas the same periodontal pathogen, *F. nucleatum*, failed to exhibit this activity. These findings suggested that *P. gingivalis* has the specific property of adhering to HNSCC cells and changing their behaviour.

A GO analysis, KEGG pathway enrichment analysis, and construction of a PPI network have been used to identify key genes and pathways involved in carcinogenesis and cancer progression.^{23,34} Geng et al. reported that L6, STAT1, LYN, BDNF, C3, CD274, PDCD1LG2 and CXCL10 were important candidates associated with OSCC using bioinformatical analyses and attempted to demonstrate that *P. gingivalis* infection promoted the initiation and progression of OSCC.³⁵ In the present study, the GO analysis extracted 16 biological processes, including the ERK1/2 cascade, response to lipopolysaccharide, regulation of cell proliferation, and negative regulation of cell migration. KEGG analyses also identified 6 pathways, including IL-17 signalling pathway, C-type lectin receptor signalling pathway, TNF signalling pathway, Leishmaniasis, Rheumatoid arthritis, and NF- κ B signalling pathway, in *P. gingivalis*-mediated HNSCC metastasis that may be relevant to *P. gingivalis* infection in HNSCC. We previously reported that *P. gingivalis* activated the ERK1/2-Ets1,

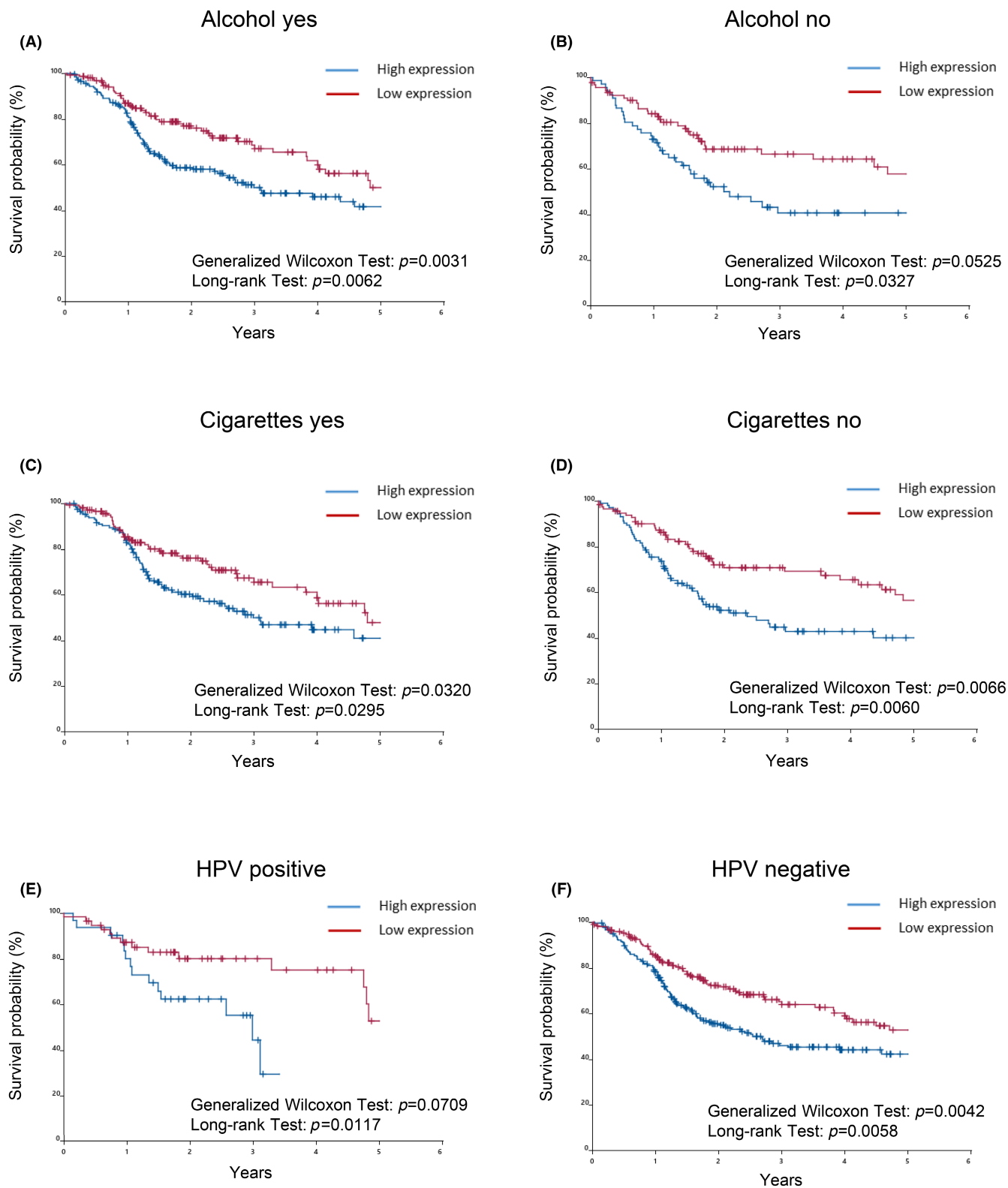


FIGURE 7 (Continued)

p38/HSP27 and PAR2/NF- κ B pathways to induce proMMP9 expression, after which the proenzyme was activated by gingipains to promote cellular invasion by HNSCC cell lines.¹⁴ The activation of these pathways was consistent with the results of the GO and KEGG enrichment pathway analyses. However, the involvement

of IL-17- and TNF- α -related pathways by *P. gingivalis* infection has yet to be demonstrated. The IL-17 family of cytokines consists of six groups: IL-17A, IL-17B, IL-17C, IL-17D, IL-17E and IL-17F, which are involved in the development of autoimmunity, inflammation, tumours, host defences against bacterial and fungal infections, and

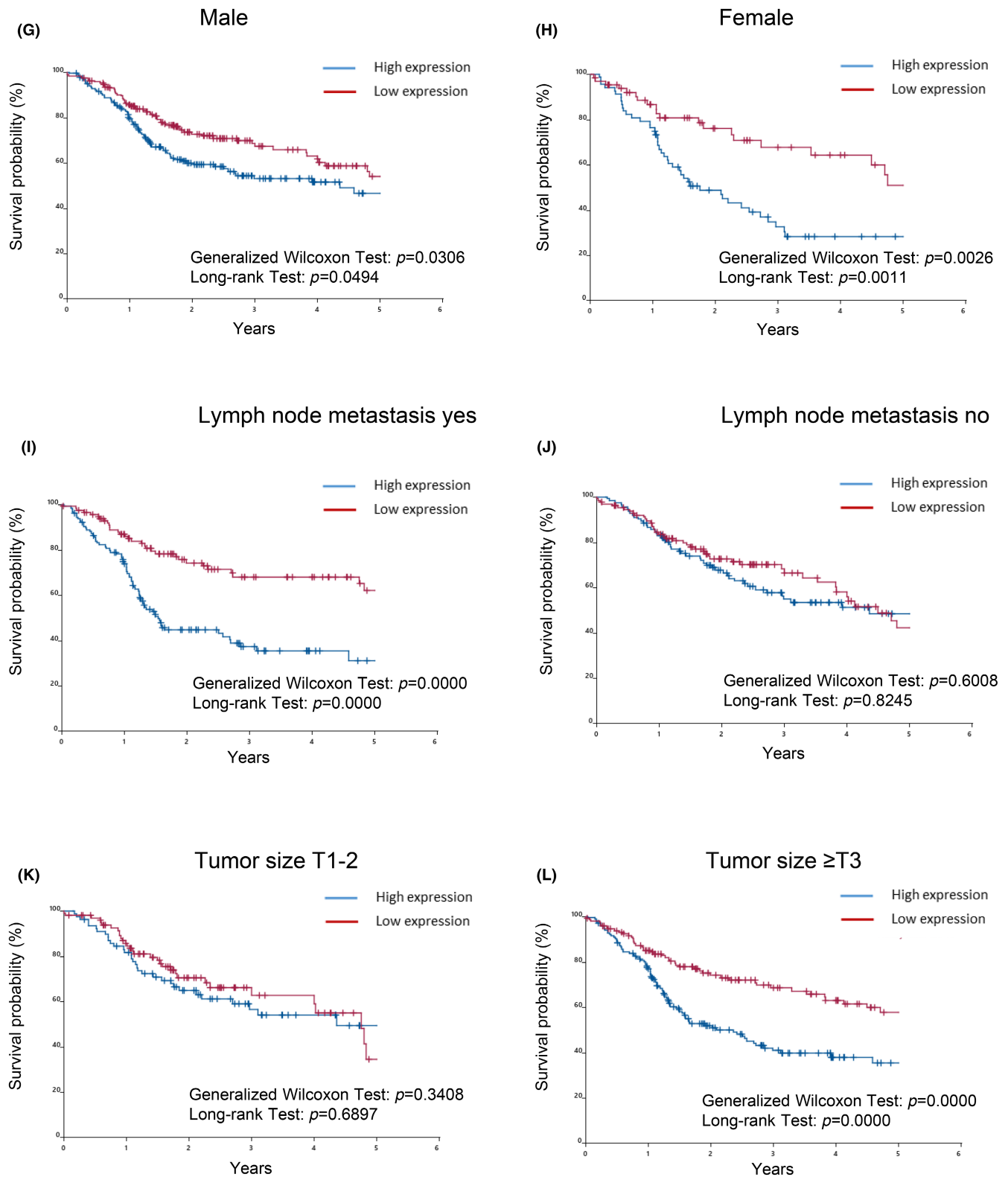


FIGURE 7 The relationship of PLAU and classical prognostic factors with survival in TCGA-HNSCC patients. The survival curve was recalculated based on the expression of PLAU, in consideration of classical prognostic factors, such as drinking, smoking, the HPV status, sex, the presence of lymph node metastasis, and tumour sizes. (A) Groups with a history of drinking. (B) Groups without a history of drinking. (C) Groups with a history of smoking. (D) Groups without a history of smoking. (E) Groups with a history of HPV infection. (F) Groups without a history of HPV infection. (G) Male group. (H) Female group. (I) Groups with lymph node metastasis. (J) Groups without lymph node metastasis. (K) Groups with tumour sizes T1-T2. (L) Groups with tumour sizes $\geq T3$.

TABLE 2 Univariate and multivariate analyses of the PLAU gene using TCGA-HNSC patient data.

	Univariate			Multivariate		
	HR	95% CI	p-value	HR	95% CI	p-value
Without the interaction mode						
PLAU_High (vs. Low)	1.722	1.294–2.293	<0.001	1.804	1.331–2.446	<0.001
Age (per 1 year)	1.016	1.003–1.029	0.015	1.023	1.009–1.038	0.001
Sex_male (vs. female)	0.721	0.535–0.973	0.032	0.873	0.620–1.228	0.434
HPV status_Positive (vs. Negative)	0.777	0.524–1.153	0.210	0.813	0.528–1.252	0.348
Drinking_history_Yes (vs. No)	0.947	0.701–1.279	0.723	1.021	0.732–1.425	0.902
Cigarettes per day_>0 (vs. 0)	0.960	0.724–1.272	0.774	0.944	0.699–1.276	0.709
M stage_m1 (vs. m0)	4.748	1.749–12.889	0.002	5.096	1.774–14.638	0.002
N stage (per 1 category)	1.078	1.002, 1.160	0.045	1.112	1.026–1.206	0.010
T stage (per 1 category)	0.999	0.902, 1.106	0.986	0.991	0.888–1.105	0.866

Note: Bold type indicates $p < 0.05$.

TABLE 3 Multivariate analyses with the interaction mode of the PLAU gene using TCGA-HNSC patient data.

	Multivariate		
	HR	95% CI	p-value
With the interaction mode [PLAU × Lymph node metastasis]			
Age (per 1 year)	1.019	1.005–1.033	0.006
Sex_male (vs. female)	0.832	0.607–1.141	0.254
M stage_m1 (vs. m0)	3.231	1.169–8.932	0.024
Lymph node metastasis. yes (vs. no)	0.739	0.459–1.190	0.213
PLAU_High (vs. Low) [in lymph node metastasis_yes]	2.908	1.864–4.536	<0.001
PLAU_High (vs. Low) [in lymph node metastasis_no]	1.189	0.789–1.792	0.407
PLAU × lymph node metastasis	2.445	1.336–4.474	0.004
With the interaction mode [PLAU × tumour size]			
Age (per 1 year)	1.018	1.005–1.032	0.007
Sex_male (vs. female)	0.766	0.560–1.049	0.097
M stage_m1 (vs. m0)	4.587	1.666–12.626	0.003
Tumour size_ ≥ T3 (vs. T1-2)	0.779	0.490–1.240	0.293
PLAU_High (vs. Low) [in tumour size_ ≥ T3]	2.298	1.595–3.312	<0.001
PLAU_High (vs. Low) [in tumour size_ < T3]	1.043	0.629–1.728	0.870
PLAU × tumour size_ ≥ T3	2.204	1.182–4.109	0.013

Note: Confounding factors to be corrected for in this analysis are background factors that were significant in the multivariate analysis in Table 2 (age, sex and the M stage). Bold type indicates $p < 0.05$.

mucosal host defence mechanisms.^{36,37} In the present study, IL-17 production was increased by *P. gingivalis* infection (Figure 5B). This result suggests that *P. gingivalis* infection activates IL-17 pathways, leading to the development of and metastasis by HNSCC. CCL20 has been reported to indirectly promote tumour progression by recruiting Treg, Th17 and Th22 cells in order to maintain a microenvironment of development and immunosuppression.^{38,39} CCL20 was also found to be associated with *P. gingivalis* infection in HNSCC.

PLAU, also known as urokinase-type plasminogen activator, is a serine protease involved in tissue remodelling and cell migration.^{40,41} PLAUI is considered to play an important role in wound healing, neuronal migration, and vascular remodelling.^{42,43}

Furthermore, in malignant tumours, PLAUI is involved in tumorigenesis, progression, cell invasion, and angiogenesis.^{40,42} The higher expression of PLAUI is regarded as a poor prognostic marker in aggressive breast cancer, hepatocellular carcinoma, and gastric cancer.^{44–46} In the present study, we identified genes related to *P. gingivalis*-induced migration, including 12 up- or 5 down-regulated genes, by an in vitro assay using the TCGA database. Moreover, CCL20 and PLAUI were suggested by the Kaplan–Meier method. PLAUI has been associated with the prognosis of patients with head and neck cancer.^{47–50} In a HNSCC bioinformatics study, PLAUI, SERPINE1, and ACTA1 were linked to the prognosis of patients. Among them, the labelling score of PLAUI significantly

increased from well ($106.78 \pm 37.323\%$) through to moderately ($182.40 \pm 6.450\%$) and poorly differentiated HNSCC samples ($272.50 \pm 36.812\%$).⁴⁷ Immunohistochemical staining revealed that PLAU was expressed mainly in the cytoplasm, with increased expression in HNSCC compared to normal oral mucosa.⁴⁷ In addition, the up-regulated expression of PLAU was associated with HPV positivity and the neck node status.⁵⁰ ITGA5, PLAU, PLAUR, SERPINE1 and TGFB1 have potential as prognostic biomarkers for HNSCC mediated by HPV infection.⁴⁸ Expression of PLAU in HNSCC was also detected by immunohistochemical staining. These previous studies and the present study demonstrate the importance of PLAU in HNSCC. However, this study is probably the first to show that PLAU is one of the genes whose expression is up-regulated in the pathway where *P. gingivalis* infection increases HNSCC cell motility and is a candidate biomarker for decreased survival in HNSCC patients. Although PLAU has been associated with a malignant status, the activation of the PLAU proteolytic cascade has been implicated in alveolar bone loss in *P. gingivalis*-mediated periodontal disease.⁵¹ In the present study, we attempt to detect changes in PLAU protein expression due to *P. gingivalis* infection and found a transient increase of PLAU protein (Figure 6A). However, no significant increase was observed in HSC-3 cells. The higher baseline levels of PLAU in HSC-3 cells may make it difficult to detect changes in PLAU protein. Previously, we reported that proMMP-9 was produced and activated in SAS cells infected with *P. gingivalis*, but not other oral SCC cell line.¹⁴ These findings indicate the heterogeneity of HNSCC cells, which may result in the different behaviour of each HNSCC cell line against specific bacteria. Nevertheless, it is clear that the findings with SAS cells provide valuable clues to begin investigating candidate of prognostic biomarkers through the TCGA HNSCC database. To correlate in vitro findings in HNSCC cell lines with those in TCGA tumour samples, it is better to infect HNSCC sample tissue with *P. gingivalis* and compare gene expression in infected and uninfected tumour tissues. Future experiments using such an experimental model will provide information on the response of HNSCC tumours to *P. gingivalis* and will help to validate in vitro studies with HNSCC cell lines.

The etiological factors correlating with HNSCC include tobacco use, alcohol consumption, and HPV infection.^{22,52} In addition, lymph node metastasis and tumour size have been associated with its prognosis.⁵³ We investigated the relationship between PLAU and these factors, such as drinking, smoking, the HPV status, sex, the presence of lymph node metastasis and tumour size, because the expression level of PLAU was also confirmed by an immunoblot analysis. The univariate analysis showed a higher risk of all-cause mortality in the high PLAU expression group than in the low PLAU expression group. Among known risk factors, age, sex, the M stage and N stage correlated with all-cause mortality. The multivariate analysis to correct for confounding factors showed that high PLAU expression was a significant risk factor for all-cause mortality even after adjusting for known risk factors. The interaction analysis with lymph node metastasis identified PLAU expression as a significant factor affecting

all-cause mortality only in the population with lymph node metastasis. The interaction analysis with tumour size also showed that PLAU expression was a significant factor affecting all-cause mortality only in the population with a large tumour size ($\geq T3$), and the interaction term was also significant. These results suggest that PLAU is a prognostic factor, similar to the M stage and N stage. Survival rates for patients with no lymph node metastases or T1-2 tumours, regardless of PLAU expression, were equivalent to those of patients with low PLAU expression and large tumours or lymph node metastases (Figure 7I-L). Therefore, if PLAU expression due to *P. gingivalis* infection is down-regulated, the risk of death in patients with advanced cancer may be reduced to that in patients with T1-2 tumours or without lymph node metastases. These findings indicate the possibility that PLAU serve as a candidate prognostic biomarker for HNSCC patients infected with *P. gingivalis*. Future clinical studies are expected to determine whether oral hygiene is related to the efficacy of treatment of HNSCC in the PLAU high-expression group, and what happens to PLAU expression when oral hygiene is improved.

In conclusion, Kaplan-Meier and Cox analyses of PLAU expression with *P. gingivalis* infection showed the potential of PLAU as a molecular prognostic marker in advanced HNSCC patients with tumour sizes $\geq T3$ or advanced HNSCC patients with lymph node metastases. Further in vivo and in vitro studies are needed to verify the findings of this study.

AUTHOR CONTRIBUTIONS

Masakazu Hamada: Conceptualization (equal); data curation (equal); formal analysis (equal); funding acquisition (equal); investigation (equal); methodology (equal); validation (equal); visualization (equal); writing – original draft (equal); writing – review and editing (equal). **Hiroaki Inaba:** Conceptualization (equal); data curation (equal); formal analysis (equal); funding acquisition (equal); investigation (equal); methodology (equal); validation (equal); visualization (equal); writing – original draft (equal); writing – review and editing (equal). **Kyoko Nishiyama:** Formal analysis (equal); funding acquisition (equal); investigation (equal); methodology (equal); visualization (equal); writing – review and editing (equal). **Sho Yoshida:** Formal analysis (equal); investigation (equal); methodology (equal); writing – review and editing (equal). **Yoshiaki Yura:** Conceptualization (equal); formal analysis (equal); methodology (equal); supervision (equal); writing – original draft (equal); writing – review and editing (equal). **Michiyo Matsumoto-Nakano:** Conceptualization (equal); formal analysis (equal); supervision (equal); writing – review and editing (equal). **Narikazu Uzawa:** Conceptualization (equal); formal analysis (equal); supervision (equal); writing – review and editing (equal).

ACKNOWLEDGMENTS

This work was supported in part by a Grant-in Aid for Scientific Research from the Japan Society for the Promotion of Science (No. 20K09918, No. 21K10111 and No. 22K17202). We also thank Subio Inc. and BIKEN Biomix Inc. for sequencing and technical support and SATISTA Inc. for statistical analyses.

CONFLICT OF INTEREST STATEMENT

The authors declare no conflicts of interest.

DATA AVAILABILITY STATEMENT

The data are available from the corresponding author upon reasonable request.

ORCID

Masakazu Hamada  <https://orcid.org/0009-0005-4522-9663>

REFERENCES

1. Al Qaraghuli MM. Biotherapeutic antibodies for the treatment of head and neck cancer: current approaches and future considerations of Photothermal therapies. *Front Oncol*. 2020;10:559596.
2. Wang C, Dickie J, Sutavani RV, Pointer C, Thomas GJ, Savelyeva N. Targeting head and neck cancer by vaccination. *Front Immunol*. 2018;9:830.
3. Yang B, Fu L, Xu S, Xiao J, Li Z, Liu Y. A nomogram based on a gene signature for predicting the prognosis of patients with head and neck squamous cell carcinoma. *Int J Biol Markers*. 2019;34:309-317.
4. McDermott JD, Bowles DW. Epidemiology of head and neck squamous cell carcinomas: impact on staging and prevention strategies. *Curr Treat Options in Oncol*. 2019;20:43.
5. Koteluk O, Bielicka A, Lemańska Ż, et al. The landscape of transmembrane protein family members in head and neck cancers: their biological role and diagnostic utility. *Cancers (Basel)*. 2021;13:13.
6. Sasazuki S, Inoue M, Iwasaki M, et al. Effect of helicobacter pylori infection combined with CagA and pepsinogen status on gastric cancer development among Japanese men and women: a nested case-control study. *Cancer Epidemiol Biomarkers Prev*. 2006;15:1341-1347.
7. Palrasu M, Zaika E, Paulrasu K, et al. Helicobacter pylori pathogen inhibits cellular responses to oncogenic stress and apoptosis. *PLoS Pathog*. 2022;18:e1010628.
8. Alexander SM, Retnakumar RJ, Chouhan D, et al. Helicobacter pylori in human stomach: the inconsistencies in clinical outcomes and the probable causes. *Front Microbiol*. 2021;12:713955.
9. Peters BA, Wu J, Pei Z, et al. Oral microbiome composition reflects prospective risk for esophageal cancers. *Cancer Res*. 2017;77:6777-6787.
10. Gao S, Li S, Ma Z, et al. Presence of Porphyromonas gingivalis in esophagus and its association with the clinicopathological characteristics and survival in patients with esophageal cancer. *Infect Agent Cancer*. 2016;11:3.
11. Wang X, Jia Y, Wen L, et al. Porphyromonas gingivalis promotes colorectal carcinoma by activating the hematopoietic NLRP3 Inflammasome. *Cancer Res*. 2021;81:2745-2759.
12. Yoshihara T, Kioi M, Baba J, et al. A prospective interventional trial on the effect of periodontal treatment on Fusobacterium nucleatum abundance in patients with colorectal tumours. *Sci Rep*. 2021;11:23719.
13. Chen WD, Zhang X, Zhang YP, et al. Fusobacterium Nucleatum is a risk factor for metastatic colorectal cancer. *Curr Med Sci*. 2022;42:538-547.
14. Inaba H, Sugita H, Kuboniwa M, et al. Porphyromonas gingivalis promotes invasion of oral squamous cell carcinoma through induction of proMMP9 and its activation. *Cell Microbiol*. 2014;16:131-145.
15. Inaba H, Amano A, Lamont RJ, Murakami Y. Involvement of protease-activated receptor 4 in over-expression of matrix metalloproteinase 9 induced by Porphyromonas gingivalis. *Med Microbiol Immunol*. 2015;204:605-612.
16. Inaba H, Tagashira M, Kanda T, Murakami Y, Amano A, Matsumoto-Nakano M. Apple- and hop-polyphenols inhibit Porphyromonas gingivalis-mediated precursor of matrix Metalloproteinase-9 activation and invasion of Oral squamous cell carcinoma cells. *J Periodontol*. 2016;87:1103-1111.
17. Ha NH, Park DG, Woo BH, et al. Porphyromonas gingivalis increases the invasiveness of oral cancer cells by upregulating IL-8 and MMPs. *Cytokine*. 2016;86:64-72.
18. Stransky N, Egloff AM, Tward AD, Kostic AD, Cibulskis K, Sivachenko A. The mutational landscape of head and neck squamous cell carcinoma. *Science*. 2011;333:1157-1160.
19. Agrawal N, Frederick MJ, Pickering CR, Bettegowda C, Chang K, Li RJ. Exome sequencing of head and neck squamous cell carcinoma reveals inactivating mutations in NOTCH1. *Science*. 2011;333:1154-1157.
20. Lawrence MS, Stojanov P, Polak P, et al. Mutational heterogeneity in cancer and the search for new cancer-associated genes. *Nature*. 2013;499:214-218.
21. Weiss J, Hayes DN. Classifying squamous cell carcinoma of the head and neck: prognosis, prediction and implications for therapy. *Expert Rev Anticancer Ther*. 2014;14:229-236.
22. Comprehensive genomic characterization of head and neck squamous cell carcinomas. *Nature*. 2015;517:576-582.
23. Hamada M, Inaba H, Nishiyama K, et al. Prognostic association of starvation-induced gene expression in head and neck cancer. *Sci Rep*. 2021;11:19130.
24. Inaba H, Nomura R, Kato Y, et al. Adhesion and invasion of gingival epithelial cells by Porphyromonas gulae. *PLoS One*. 2019;14:e0213309.
25. Subio x Omics. <https://www.subioplatform.com>.
26. National Cancer Institute. Genomic Data Commons Data Portal. <https://portal.gdc.cancer.gov>
27. Liu D, Liu S, Liu J, Miao L, Zhang S, Pan Y. sRNA23392 packaged by Porphyromonas gingivalis outer membrane vesicles promotes oral squamous cell carcinomas migration and invasion by targeting desmocollin-2. *Mol Oral Microbiol*. 2021;36:182-191.
28. Zhu C, Menyhart O, Györfy B, He X. The prognostic association of SPAG5 gene expression in breast cancer patients with systematic therapy. *BMC Cancer*. 2019;19:1046.
29. Shimizu H, Nakayama KI. A 23 gene-based molecular prognostic score precisely predicts overall survival of breast cancer patients. *EBioMedicine*. 2019;46:150-159.
30. Tuominen H, Rautava J. Oral microbiota and cancer development. *Pathobiology*. 2021;88:116-126.
31. Michaud DS, Lu J, Peacock-Villada AY, et al. Periodontal disease assessed using clinical dental measurements and cancer risk in the ARIC study. *J Natl Cancer Inst*. 2018;110:843-854.
32. Tezal M, Sullivan MA, Reid ME, et al. Chronic periodontitis and the risk of tongue cancer. *Arch Otolaryngol Head Neck Surg*. 2007;133:450-454.
33. Ahn J, Segers S, Hayes RB. Periodontal disease, Porphyromonas gingivalis serum antibody levels and orodigestive cancer mortality. *Carcinogenesis*. 2012;33:1055-1058.
34. Xu Y, Kong D, Li Z, Qian L, Li J, Zou C. Screening and identification of key biomarkers of papillary renal cell carcinoma by bioinformatic analysis. *PLoS One*. 2021;16:e0254868.
35. Geng F, Wang Q, Li C, et al. Identification of potential candidate genes of Oral cancer in response to chronic infection with Porphyromonas gingivalis using Bioinformatical analyses. *Front Oncol*. 2019;9:91.
36. Iwakura Y, Ishigame H, Saijo S, Nakae S. Functional specialization of interleukin-17 family members. *Immunity*. 2011;34:149-162.
37. Song X, Qian Y. IL-17 family cytokines mediated signaling in the pathogenesis of inflammatory diseases. *Cell Signal*. 2013;25:2335-2347.
38. Lv X, Yu X. Signatures and prognostic values of related immune targets in tongue cancer. *Front Surg*. 2022;9:952389.

39. Wu N, Wang Y, Wang K, et al. Cathepsin K regulates the tumor growth and metastasis by IL-17/CTSK/EMT axis and mediates M2 macrophage polarization in castration-resistant prostate cancer. *Cell Death Dis.* 2022;13:813.
40. Gao Y, Ma X, Lu H, Xu P, Xu C. PLAU is associated with cell migration and invasion and is regulated by transcription factor YY1 in cervical cancer. *Oncol Rep.* 2023;49:25.
41. Crippa MP. Urokinase-type plasminogen activator. *Int J Biochem Cell Biol.* 2007;39:690-694.
42. Yu T, Liu J, Wang Y, et al. METTL3 promotes colorectal cancer metastasis by stabilizing PLAU mRNA in an m6A-dependent manner. *Biochem Biophys Res Commun.* 2022;614:9-16.
43. Ismail AA, Shaker BT, Bajou K. The plasminogen-activator plasmin system in physiological and pathophysiological angiogenesis. *Int J Mol Sci.* 2021;23:337.
44. Moquet-Torcy G, Tolza C, Piechaczyk M, Jariel-Encontre I. Transcriptional complexity and roles of Fra-1/AP-1 at the uPA/Plau locus in aggressive breast cancer. *Nucleic Acids Res.* 2014;42:11011-11024.
45. Sun J, Zhou F, Xue J, Ji C, Qu Y, Pan Y. Long non-coding RNA TRPM2-AS regulates microRNA miR-138-5p and PLAU (plasminogen activator, Urokinase) to promote the progression of gastric adenocarcinoma. *Bioengineered.* 2021;12:9753-9765.
46. Tsai MC, Yen YH, Chang KC, et al. Elevated levels of serum urokinase plasminogen activator predict poor prognosis in hepatocellular carcinoma after resection. *BMC Cancer.* 2019;19:1169.
47. Yang K, Zhang S, Zhang D, et al. Identification of SERPINE1, PLAU and ACTA1 as biomarkers of head and neck squamous cell carcinoma based on integrated bioinformatics analysis. *Int J Clin Oncol.* 2019;24:1030-1041.
48. Zhou Q, Yuan O, Cui H, et al. Bioinformatic analysis identifies HPV-related tumor microenvironment remodeling prognostic biomarkers in head and neck squamous cell carcinoma. *Front Cell Infect Microbiol.* 2022;12:1007950.
49. Zhang G, Li T, Tan G, et al. Identity of MMP1 and its effects on tumor progression in head and neck squamous cell carcinoma. *Cancer Med.* 2022;11:2516-2530.
50. Li Z, Chen C, Wang J, et al. Overexpressed PLAU and its potential prognostic value in head and neck squamous cell carcinoma. *PeerJ.* 2021;9:e10746.
51. Fleetwood AJ, O'Brien-Simpson NM, Veith PD, et al. Porphyromonas gingivalis-derived RgpA-Kgp complex activates the macrophage Urokinase plasminogen activator system: IMPLICATIONS FOR PERIODONTITIS. *J Biol Chem.* 2015;290:16031-16042.
52. Damasio MPS, Nascimento CS, Andrade LM, de Oliveira VL, Calzavara-Silva CE. The role of T-cells in head and neck squamous cell carcinoma: from immunity to immunotherapy. *Front Oncol.* 2022;12:1021609.
53. Chiesa-Estomba CM, Lechien JR, Ayad T, et al. Clinical and histopathological risk factors for distant metastasis in head and neck cancer patients. *Acta Otorhinolaryngol Ital.* 2021;41:6-17.

How to cite this article: Hamada M, Inaba H, Nishiyama K, et al. Transcriptomic analysis of *Porphyromonas gingivalis*-infected head and neck cancer cells: Identification of PLAU as a candidate prognostic biomarker. *J Cell Mol Med.* 2024;00:1-18. doi:[10.1111/jcmm.18167](https://doi.org/10.1111/jcmm.18167)